

# Scaling of the Hall coefficient and resistivity in underdoped and overdoped $R\text{Ba}_2\text{Cu}_3\text{O}_y$ films

N. Y. Chen, V. C. Matijasevic, and J. E. Mooij

*Applied Physics, Delft University of Technology, Lorentzweg 1, 2628 CJ Delft, The Netherlands*

D. van der Marel

*Department of Physics, University of Groningen, Nijenborgh 4, 9747 AG Groningen, The Netherlands*

(Received 7 July 1994)

We have studied the normal-state transport properties, the resistivity  $\rho(T)$ , and the Hall coefficient  $R_H(T)$  on two sets of samples of  $R\text{Ba}_2\text{Cu}_3\text{O}_y$  compounds ( $R = \text{Y}, \text{Sm}$ ) away from optimal doping. In the overdoped regime,  $R_H(T)$  obtained from Ca-doped  $\text{SmBa}_2\text{Cu}_3\text{O}_y$  shows a saturation at high temperature. While  $R_H(T)$  decreases with  $T$  at low temperature, it becomes temperature independent when the temperature exceeds a certain value  $T_H^*$ . This characteristic  $T_H^*$  decreases with doping, and is only visible in our experimental temperature range when the samples are sufficiently doped. By assuming a universal functional form for all doping levels, the temperature dependence of the Hall coefficient can be scaled. Another characteristic temperature  $T_\rho^*$  can be seen from the resistivity data in the underdoped regime, obtained from the oxygen-deficient  $\text{YBa}_2\text{Cu}_3\text{O}_y$  samples. Above  $T_\rho^*$ ,  $\rho(T)$  increases almost linearly with  $T$ , whereas below, it deviates from the linear behavior. We discuss the relationship between these two characteristic temperatures  $T_H^*$  and  $T_\rho^*$  for different doping levels. For the underdoped samples, the resistivity is fitted well by the relation  $\rho(T) \approx aR_H(T)T^2 + b$ .

The normal-state properties of the cuprate high- $T_c$  superconductors, observable at temperatures above the superconducting transition  $T_c$ , have enjoyed an increasing amount of attention in recent years. This is in addition to the high  $T_c$ 's found in these materials, which was initially the most fascinating topic for the majority of research. The normal-state transport properties, such as the resistivity  $\rho(T)$  and the Hall coefficient  $R_H(T)$ , exhibit anomalous temperature dependences (i.e., non-Fermi-liquid behavior), which by themselves are at least as fascinating as the high superconducting transition temperatures. It may be that the underlying mechanisms for these intriguing properties are related to each other.

The resistivity in these materials when optimally doped (for the highest  $T_c$ ) generally increases linearly with temperature. At the same time, the Hall coefficient has a temperature dependence of approximately  $1/T$ . Deviation from this behavior becomes increasingly apparent when the materials are further away from optimum doping. Most of the experiments on the  $R\text{Ba}_2\text{Cu}_3\text{O}_y$  cuprates ( $R = \text{Y}$ , lanthanides) were done in the underdoped regime (hole doping less than optimal) on oxygen-deficient  $\text{YBa}_2\text{Cu}_3\text{O}_y$  (YBCO) thin films or single crystals. In our work, we try to obtain a more complete picture of this subject by extending our study into the overdoped regime on Ca-doped  $\text{SmBa}_2\text{Cu}_3\text{O}_y$  (SBCO) thin films, and compare them to our oxygen-deficient YBCO samples. Recently Ito *et al.*<sup>1</sup> and Hwang *et al.*<sup>2</sup> have shown for different sets of high- $T_c$  cuprates that the normal-state properties can be scaled as a function of doping in either the underdoped or the overdoped regimes. We find that the scaling relationship for  $R_H(T)$  can be extended to all doping levels of our samples, from the overdoped into the underdoped regime.

We have grown our YBCO thin films on  $5 \times 5 \text{ mm}^2$  (100)  $\text{SrTiO}_3$  substrates by laser ablation at  $750^\circ\text{C}$  and 1 mbar oxygen pressure. X-ray diffraction measurement showed that

they are  $c$ -axis oriented. No minority phases were observed. The  $T_c$ 's of the as-made samples were around 91 K with sharp transitions ( $\Delta T_c < 2 \text{ K}$ ). The resistivity for several samples varies from 180 to  $390 \mu\Omega \text{ cm}$  at 300 K. In order to study the underdoped regime, three samples have been repeatedly annealed at reduced oxygen pressures (1 mbar  $< p_{\text{O}_2} < 1 \text{ bar}$ ) at  $450^\circ\text{C}$ . Two of the samples failed to give reproducible values for  $T_c$  and resistivity after annealing back to the original fully oxygenated state. Therefore, we present only the data from one YBCO sample that survived all anneals, also the one with the lowest resistivity. The  $T_c$  of this sample could be restored to its original as-made value after 11 annealing runs with a small increase (0.5 K), accompanied by a slightly increased resistivity (10%). Our Ca-doped  $\text{Sm}_{1-x}\text{Ca}_x\text{Ba}_2\text{Cu}_3\text{O}_y$  thin films were grown by co-evaporation in a MBE deposition system. Films were grown in an ozone beam and at  $750^\circ\text{C}$ . By adjusting the relative evaporation rates for different elements to the desired ratio, samples with three different levels of doping ( $x = 0.1, 0.2, 0.4$ ) were made. Ca doping of the structure has been shown to lead to hole overdoping of the plane layers.<sup>3,4</sup> Low oxygen pressure annealing of the Ca-doped samples showed us that the  $T_c$  increases upon reduction and that therefore the samples are overdoped compared with optimal hole doping. We find a solid solubility regime of Ca doping for our films up to 0.3–0.4 Ca substitution.<sup>5</sup>

The in-plane resistivity and Hall coefficient were measured using the van der Pauw technique without patterning. Four Au pads (diameter  $\approx 0.5 \text{ mm}$ ) were laser ablated on the corners of the sample through an aluminum foil mask in vacuum at room temperature. This was done to ensure good electrical contact between the samples and the contact pins. For each sample,  $\rho$  and  $R_H$  were measured as a function of temperature in a liquid helium flow cryostat during two sepa-

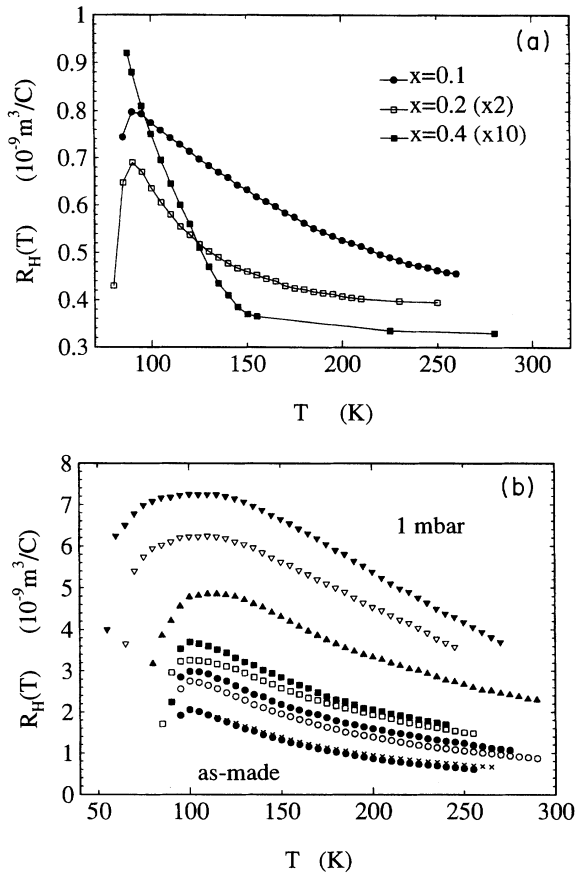


FIG. 1. The Hall coefficient ( $R_H$ ) for (a) overdoped  $\text{Sm}_{1-x}\text{Ca}_x\text{Ba}_2\text{Cu}_3\text{O}_y$  samples and (b) underdoped oxygen-deficient  $\text{YBa}_2\text{Cu}_3\text{O}_y$ . The Hall coefficient in (a) is multiplied by factors 2 and 10, for the 0.2 and 0.4 Ca-doped samples, respectively. The curves in (b) are for various oxygen anneals from 1 bar to 1 mbar going upward.

rate runs. For the Hall measurements a magnetic field of 0.6 T was applied perpendicular to the film.

In the overdoped regime  $R_H$  decreases with increasing temperature; see Fig. 1(a). At higher doping levels ( $x=0.2, 0.4$ ) a characteristic temperature  $T_H^*$  can be seen. Above the temperature  $T_H^*$ , which decreases with increasing doping level,  $R_H(T)$  becomes almost temperature independent. Hwang *et al.* reported earlier the existence of  $R_H(T)$  saturation in overdoped  $\text{La}_{2-x}\text{Sr}_x\text{CuO}_4$  (LSCO) at high temperatures.<sup>2</sup> Here we report this behavior for the  $\text{RBa}_2\text{Cu}_3\text{O}_y$  compound as well.

Figure 1(b) shows the  $R_H(T)$  of the YBCO film measured before and after various low oxygen pressure annealing runs. In most of the underdoped cases, except the ones with the lowest doping (top three lines),  $R_H$  decreases with increasing temperature in the whole range of measurements, and follows roughly  $1/T$ . The deviation from this behavior can be observed for the lowest doping levels at low temperature, where  $R_H$  initially increases with temperature (above  $T_c$ ) to a maximum value and subsequently decreases. Ito *et al.* observed that this deviation followed exactly the excess conductivity found at low temperatures in the underdoped samples.<sup>1</sup> Our data confirm the observation by Ito *et al.* It

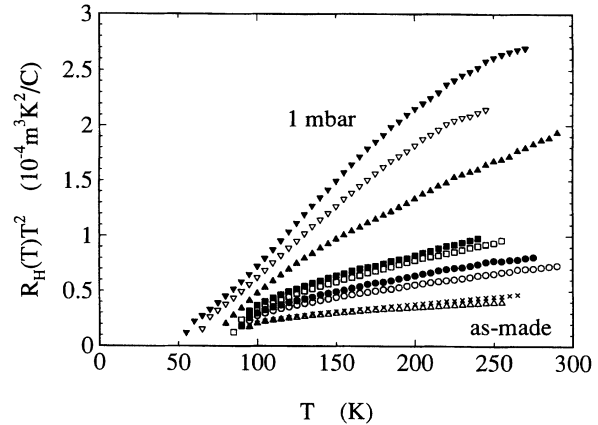


FIG. 2.  $R_H(T)T^2$  vs temperature. The Hall data presented in this way are very similar to the resistivity data.

becomes even more obvious when we plot  $R_H(T)T^2$ , shown in Fig. 2 for the underdoped samples. These curves have the same features as do the resistivity curves for these samples. By choosing corresponding constants  $a$  and  $b$  for each doping level, the set of  $\rho(T)$  and  $R_H(T)T^2$  curves can be fitted onto each other using the relation.

$$\rho_{\text{cal}}(T) = aR_H(T)T^2 + b. \quad (1)$$

Figure 3(a) compares  $\rho(T)$  data (solid lines) and the fitted  $\rho_{\text{cal}}(T)$  from the  $R_H(T)$  data (circles) for the underdoped samples. The two sets of curves fall well onto each other, if one disregards the differences at higher temperature in the two least doped cases. In the inset of Fig. 3(a) we show the ratio of this set of curve pairs. At this point, we would like to mention two interesting features concerning the relationship between  $\rho(T)$  and  $R_H(T)$ . First of all, this relationship which we find for the underdoped regime is similar, but slightly different from the one proposed by Anderson<sup>6</sup> for the Hall angle in a Luttinger liquid,  $\cot(\theta_H) = \rho/(HR_H) = \alpha T^2 + C$  and first observed by Chien *et al.*<sup>7</sup>  $H$  is the magnetic field and  $\alpha$  and  $C$  are constants. The reason that our data fit better to our Eq. (1) than to the Anderson equation may be due to the fact that our  $\rho(T)$  curves do not extrapolate to zero at zero kelvin.<sup>8</sup> The value of  $a$ , comparable to  $\alpha$  in Anderson's relation, decreases monotonically with decreasing doping level in our data. This is in agreement with the results reported by Wuyts *et al.*<sup>9</sup> on oxygen-deficient YBCO thin films, and other reported experiments on doped LSCO.<sup>2</sup> Different behavior has also been reported for YBCO.<sup>10,11</sup> Secondly, despite the slight downward curvature in the as-made  $\rho(T)$  curve, and the fact that it clearly does not extrapolate to zero at zero temperature,  $R_H(T)T^2$  still follows  $\rho(T)$  behavior almost exactly.

While this relationship is directly obtained by fitting the data from underdoped samples, it is interesting to see whether it is also valid for the samples in the overdoped regime, which show the  $R_H(T)$  saturation ( $x=0.2, 0.4$ ). In Fig. 3(b) we plot the temperature dependence of  $\rho(T)_{\text{cal}}$  calculated from  $R_H(T)$  data using Eq. (1) and fitted with the corresponding values of  $a$  and  $b$ , together with the actually measured  $\rho(T)$ . Although there is an upward curvature in both sets of curves, these curves do not fall onto each other.

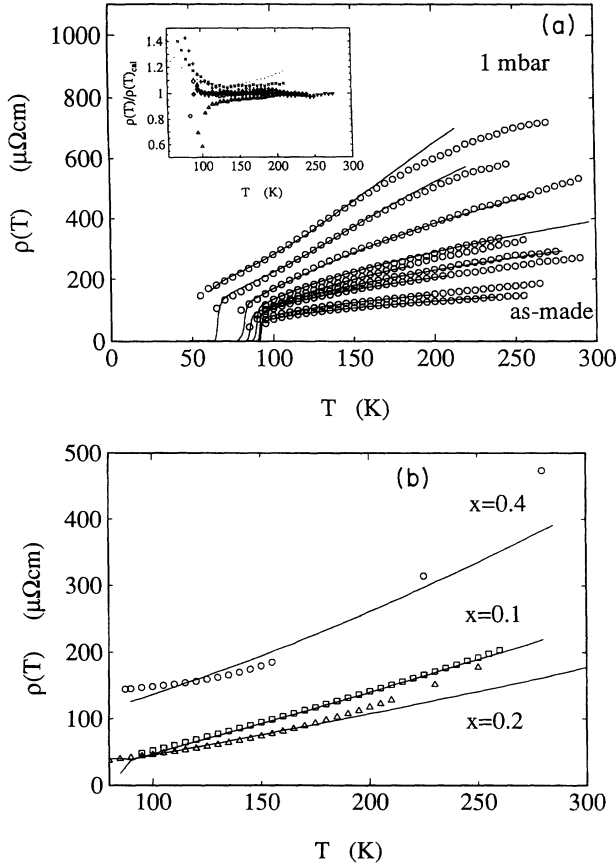


FIG. 3. A comparison of  $\rho(T)$  data (solid lines) and  $\rho_{cal}(T)$  (symbols), fitted from  $R_H(T)$  using Eq. (1) for (a) underdoped YBCO samples and (b) overdoped SBCO samples. Inset of (a) shows the ratio of the two.

Further, the resistivity does not have any characteristic temperature, as does the Hall coefficient. Instead the resistivity curves show an increasing amount of curvature as the doping increases, up to  $T^{1.6}$  for the highest doping shown here.

Hwang *et al.*<sup>2</sup> suggested that all overdoped LSCO samples have  $R_H(T)$  that can be put onto one master curve by scaling the temperature axis with the corresponding  $T^*$ , above which  $R_H$  saturates (the same temperature is denoted as  $T_H^*$  in this paper), together with an appropriate scaling and offset for  $R_H(T)$ . This master curve does not simply follow  $1/T$ . Following the suggestion of Hwang *et al.*,<sup>2</sup> we scaled all of our  $R_H(T)$  curves onto a single master curve by using independent scaling parameters,  $T_H^*$  and  $R_H^*$ , and an offset  $R_H^\infty$ . Here a functional form  $R_H^\infty + R_H^* f(T/T_H^*)$  is used, where  $f(T/T_H^*)$  is the temperature-dependent part of  $R_H(T)$ . Parameters  $T_H^*$  and  $R_H^*$  are arbitrary to a constant factor. We chose to define them in the same manner as Hwang *et al.*, i.e., we have used the linear extrapolation of the master curve to 0 K for the definition of  $R_H^*$  and the intercept of the high temperature  $R_H^\infty$  with the linear extrapolation of  $R_H(T)$  from low temperature as the definition of  $T_H^*$ . We find that  $T_H^*$  for the  $R\text{Ba}_2\text{Cu}_3\text{O}_y$  compound defined in this manner, gives half the value reported by Hwang *et al.* for the LSCO compound. In our case, the resulting master curve also does not simply follow  $1/T$ ; see Fig. 4.

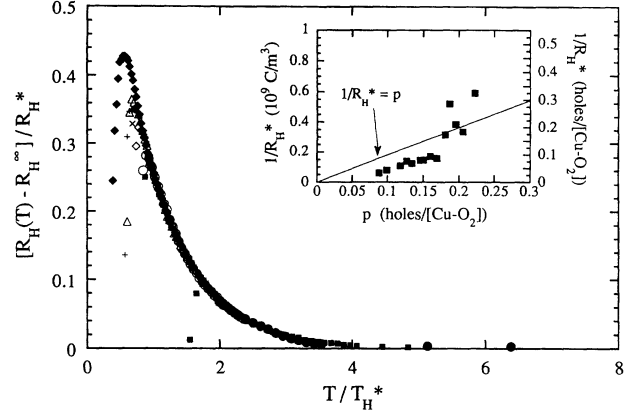


FIG. 4. The Hall coefficient rescaled as  $[R_H(T) - R_H^\infty]/R_H^*$  vs  $T/T_H^*$ . The scaling was done in a manner similar to Ref. 2. This master curve seems to follow  $e^{-1.31T/T_H^*}$ . Inset:  $1/R_H^*$  as determined from the fit to the master curve, vs the hole number per copper in the copper oxygen planes determined from  $T_c$  as explained in the text. The line is drawn for  $1/R_H^* = p$ .

On the other hand, Ito *et al.*<sup>1</sup> and Wuyts *et al.*<sup>9</sup> reported that the resistivity curves for the (underdoped) oxygen-deficient YBCO can also be appropriately scaled to a master curve by dividing the temperature by a  $T_0$ , i.e., the temperature under which the resistivity deviates from linearity (denoted here as  $T_\rho^*$ ). We are also able to scale our  $\rho(T)$  curves onto a single master curve in this manner. Since  $\rho(T)$  and  $R_H(T)$  are approximately related by Eq. (1) in the underdoped regime, this implies that  $R_H(T)$  can also be scaled in the underdoped regime. In Fig. 4 we show the curves for all doping, scaled as Hwang *et al.* did for the overdoped case. In addition, because  $\rho(T)$  and  $R_H(T)$  can be fitted onto each other by Eq. (1), then  $T_\rho^*$  should differ from  $T_H^*$  only by a constant factor in the underdoped regime.

In order to plot  $T_H^*$  and  $T_\rho^*$  for both overdoped and underdoped  $R\text{Ba}_2\text{Cu}_3\text{O}_y$  samples in one figure, we calculated the number of holes per copper in the copper oxygen plane layers using a general relation for the cuprates given by Tallon,<sup>12</sup>  $T_c/T_c^{\text{max}} = 1 - 82.6 \times (p - 0.16)^2$ , based on bond valence sums.  $T_c$  is the transition temperature measured for each sample, and  $T_c^{\text{max}}$  is the highest  $T_c$  for the sample (at optimal doping,  $p = \text{holes}/[\text{Cu-O}_2] = 0.16$ ).  $T_c^{\text{max}}$  is chosen as 91.5 K for the YBCO before and after annealing in reduced oxygen pressure. For the Ca-doped SBCO samples, however, we have chosen the respective maximum  $T_c$  reached for each composition during successive low oxygen pressure anneals.

We plot  $T_\rho^*$  and  $T_H^*$  vs the number of holes per copper in the copper oxygen plane layers  $p$  in Fig. 5. The value of  $T_\rho^*$  has a relatively large uncertainty ( $\Delta T_\rho^* \sim 50$  K) due to the slight curvature in all our  $\rho(T)$  curves in the temperature range of our measurements. Both characteristic temperatures decrease with hole concentration and scale with each other well in the underdoped regime. The actual value of  $T_H^*$  depends on the manner in which it is defined from the master curve. We have used the same definition as Hwang *et al.*

$R_H(T)$  can be divided into two regions, above and below  $T_H^*$ . At low temperature ( $T_c < T < T_H^*$ ), the scaling factor  $R_H^*$  determines the doping dependence of the Hall coeffi-

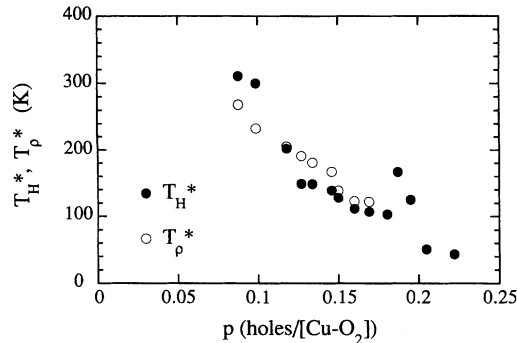


FIG. 5. Characteristic temperatures  $T_H^*$  (full circles) and  $T_\rho^*$  (open circles) derived from the Hall coefficient and resistivity data, respectively.

cient. In the high-temperature limit, however,  $R_H^\infty$  sets the value for the Hall coefficient. Both  $R_H^*$  and  $R_H^\infty$  decrease with doping. It is tempting to interpret the  $R_H^*$  as the “effective” Hall coefficient of the strongly correlated system since  $1/R_H^*$  follows the hole doping,  $p$ , rather well; see inset of Fig.

4. In fact, the vertical shift between  $1/R_H^*$  and  $p$  may be due to localized holes at low doping. At high doping, we tentatively assign the increase in the Hall number to a contribution from the free carriers in the chains.  $T_H^*$  and  $T_\rho^*$  may be related to the spin gap as suggested by Ito *et al.*<sup>1</sup> In the limit  $T \gg T_H^*$ , one gradually recovers the usual Fermi-liquid behavior. For the strongly doped samples this is further manifested by a curvature in the resistivity, as seen in Fig. 3(b), which approaches the  $T^2$  behavior predicted for a Fermi liquid.

In conclusion, we have found that the Hall coefficient of  $\text{RbBa}_2\text{Cu}_3\text{O}_y$  films can be scaled onto a single master curve for all doping levels, but that the resistivity scales only in the underdoped regime. The scaling factor for the Hall coefficient is closely related to the actual hole doping of the copper oxygen plane layers. For strongly doped samples, the data show a clear sign of saturation of the Hall coefficient at high temperature, as well as Fermi-liquid-like behavior for the resistivity.

We would like to thank Leo Lander, Kitty van Dijk, and Huub Appelboom for assistance. This work is supported in part by FOM and NOP.

<sup>1</sup>T. Ito, K. Takenaka, and S. Uchida, Phys. Rev. Lett. **70**, 3995 (1993).

<sup>2</sup>H. Y. Hwang, B. Batlogg, H. Takagi, H. L. Kao, J. Kwo, R. J. Cava, J. J. Krajewski, and W. F. Peck, Jr., Phys. Rev. Lett. **72**, 2636 (1994).

<sup>3</sup>Y. Tokura, J. B. Torrance, T. C. Huang, and A. I. Nazzari, Phys. Rev. B **38**, 7156 (1988).

<sup>4</sup>B. Fisher, J. Genossar, C. G. Kuper, L. Patlagan, G. M. Reisner, and A. Knizhik, Phys. Rev. B **47**, 6054 (1993).

<sup>5</sup>V. Matijasevic (unpublished).

<sup>6</sup>P. W. Anderson, Phys. Rev. Lett. **67**, 2092 (1991).

<sup>7</sup>T. R. Chien, Z. Z. Wang, and N. P. Ong, Phys. Rev. Lett. **67**, 2088 (1991).

<sup>8</sup>Even if for the optimally doped sample  $\rho(T)$  does extrapolate to 0 at 0 K, that may not be the case for the samples away from optimal doping.

<sup>9</sup>B. Wuyts, E. Osquiguil, M. Maenhoudt, S. Libbrecht, Z. X. Gao, and Y. Bruynseraede, Physica C **222**, 341 (1994).

<sup>10</sup>P. Xiong, G. Xiao, and X. D. Wu, Phys. Rev. B **47**, 5516 (1993).

<sup>11</sup>J. M. Harris, Y. F. Yan, and N. P. Ong, Phys. Rev. B **46**, 14 293 (1992).

<sup>12</sup>J. L. Tallon and N. E. Flower, Physica C **204**, 237 (1993).